*Environ. Sci. Technol.* **1998**, *32,* 2776−2781

# Partitioning of Hydrophobic Organic Compounds to Sorbed Surfactants. 2. Model Development/Predictions for Surfactant-Enhanced Remediation Applications

SEOK-OH KO AND
MARK A. SCHLAUTMAN*
*Environmental Engineering Specialty Area, Department of Civil Engineering, Texas A&M University, College Station, Texas 77843-3136*

A one-dimensional numerical model was developed to simulate the performance of surfactant-enhanced remediation (SER) applications for saturated subsurface systems containing adsorbed hydrophobic organic compounds (HOCs). The model incorporates temporally and spatially dependent HOC and surfactant mass balance equations to compute distributions in the aqueous, micellar, sorbed surfactant, and subsurface solid phases. In particular, the model accounts for losses of surfactant by sorption to the subsurface media and for the subsequent partitioning of HOCs to sorbed surfactant. Parameter values for the model were estimated from experimental rate and equilibrium data from the literature, and sensitivity analysis was conducted to evaluate the model performance and potential SER applications. Simulation results show that the relative affinity of HOCs and surfactants for the immobile subsurface solid phase (i.e., the respective retardation factors) is critical for determining whether contaminant desorption can be enhanced by surfactants. For example, under the conditions simulated here, removal of phenanthrene and naphthalene from a representative sandy (i.e., low organic carbon) aquifer is actually hindered by flushing with surfactant solutions, whereas for more hydrophobic contaminants (e.g., pyrene) surfactant addition can enhance HOC removal. Likewise, an increase in the organic carbon content of the subsurface solid phase increases the effectiveness of SER processes. The important rate and equilibrium model parameters evaluated in this study provide useful guidelines for the design and application of SER processes for contaminated subsurface systems and for interpreting SER-related studies.

## Introduction

Surfactants have been shown to be effective agents that can aid in the remediation of subsurface environments contaminated by hydrophobic organic compounds (HOCs). In general, two different treatment objectives are often considered: (1) minimizing HOC mobility by sorption to an immobile sorbed surfactant phase or (2) increasing HOC mobility by partitioning to a mobile surfactant micelle phase. For the latter case, micellar solubilization occurs when the surfactants are present at concentrations above the critical micelle concentration (cmc). Considerable effort has been made to develop in-situ surfactant-enhanced remediation (SER) processes to remove the HOCs that often exist in the sorbed state and/or are present as nonaqueous phase liquids (NAPLs) in contaminated subsurface systems because conventional pump-and-treat processes generally show only limited success for these applications (*1*−*5*).

A few one- or two-dimensional mathematical models have been developed to simulate the performance of SER processes for the removal of organic contaminants from porous media (*2, 6, 7*). In general, the target contaminants in these simulations existed not in the sorbed state but instead as NAPLs. Results from the models, when compared to laboratory column experiments, have demonstrated the importance of rate-limited mass transfer processes between the contaminants and aqueous surfactant solutions. Recently, three-dimensional models have been developed to incorporate a variety of interphase mass transfer processes, thereby allowing simulation of the transport of multicomponent species in multiphase systems (*8*).

Many of the mathematical models developed to date have neglected the effects of surfactant sorption on the removal of HOCs by SER processes, presumably because of the use of relatively high surfactant concentrations with respect to the cmc. However, the effects of surfactant sorption and the corresponding sorption of HOCs to sorbed surfactants can be critical when the target compounds exist in the adsorbed state. Previous studies of surfactant sorption on soils and soil minerals have shown that the process can continue far above the cmc of many surfactants (*1, 9, 10*). As shown in our preceding paper, sorbed surfactants can be an effective medium for HOC partitioning; this partitioning capability is highly dependent on the surfactant sorption isotherm, which generally shows a high degree of nonlinearity (*10*). In addition, HOC solubilization rates to micelles and sorbed surfactants will potentially influence remediation time scales as well as surfactant addition strategies. No studies to date, however, have reported on the modeling of surfactant-enhanced solubilization processes of adsorbed HOCs in which the effect of surfactant sorption on HOC transport has been taken into account.

The primary objectives of this study were to (1) develop an SER model that accurately predicts the effect of surfactant flushing by accounting for surfactant sorption to the subsurface media, (2) examine the importance of the rates of SER processes, and (3) demonstrate the use of this model as a tool for maximizing the efficiency of SER processes. A one-dimensional model was formulated based on mass balances of all constituents in the system. The model includes the effects of complex nonlinear sorption isotherms (e.g., ref *10*) on surfactant transport and the corresponding HOC distribution in each phase (i.e., water, micelle, sorbed surfactant, subsurface solids). Experimental data for surfactant sorption and HOC partitioning to micelles and sorbed surfactants (*10, 11*) are employed to demonstrate the relative importance of each parameter. Although the model developed here cannot be expected to perfectly simulate all contaminated sites because of their different physical and chemical characteristics, the factors evaluated should provide useful guidelines for the design of SER processes and for interpreting the results of SER-related studies.

## Model Development

A number of one-dimensional models have been developed to evaluate the transport of HOCs in subsurface systems. In

* Corresponding author phone: (409)845-3011; fax: (409)862-1542; e-mail: schlautman@tamu.edu.


S0013-936X(97)01076-6 CCC: $15.00 © 1998 American Chemical Society
Published on Web 08/12/1998

**TABLE 1. Chemical Parameters Used for Numerical Simulations of Surfactant and HOC Transport [a]**

| | compound | | | | |
|---|---|---|---|---|---|
| | phenanthrene | naphthalene | pyrene | SDS | Tween 80 |
| log $K_{ow}$ [b] | 4.57 | 3.36 | 5.17 | | |
| $K_{surf}^{min}$ (L/g) | | | | | |
| $S_{surf}$ < 90 mg/L | | | | 5.0E−4 | 2.13E−3 |
| 90 < $S_{surf}$ < 400 mg/L | | | | 6.1E−3 | |
| 400 mg/L < $S_{surf}$ | | | | 3.0E−4 | |
| $K_{HOC}^{mic}$ for SDS (L/g) | 7.924 | 1.093 | 96.2[c] | | |
| $K_{HOC}^{mic}$ for Tween 80 (L/g) | 41.99 | 2.102 | ND[d] | | |
| $K_{HOC}^{ss}$ for SDS (L/g) | 47.93 | 1.823 | 347.2[e] | | |
| $K_{HOC}^{ss}$ for Tween 80 (L/g) | 43.93 | 2.593 | ND | | |
| $K_{HOC}^{min}$ (L/g) | 4.11E−4 | 7.28E−5 | 9.69E−3[f] | | |
| $k_f^{surf}$ ($s^{-1}$) for SDS and Tween 80 | | | | 9.78E−3 | 9.78E−3 |
| $k_{f,HOC}^{mic}$ ($s^{-1}$) | 1.31E−5 | 1.55E−5[g] | 1.22E−5[g] | | |
| $k_{f,HOC}^{ss}$ ($s^{-1}$) | 4.38E−5 | 5.18E−5[g] | 4.08E−5[g] | | |
| $k_{f,HOC}^{min}$ ($s^{-1}$) | 1.39E−3[h] | 1.39E−3[h] | 1.39E−3[h] | | |

[a] Values are from ref 10 unless otherwise noted. [b] Reference 18. [c] From ref 11. [d] ND, not determined. [e] Estimated from a correlation between log $K_{ow}$ and log $K_{ss}$. [f] Estimated from ref 19. [g] Obtained by multiplying the ad/solubilization rate of phenanthrene and the ratio of molecular diffusivity of phenanthrene and naphthalene (or pyrene). [h] Estimated from ref 20.

the formulation of a transport model that includes flushing with a surfactant solution, mass balance equations must incorporate the multiple chemical species (i.e., HOC, surfactant) present in the multiple phases present (i.e., aqueous, micellar, sorbed surfactant, subsurface solids). This system of mass balance equations is similar to those used to evaluate the transport of contaminants in the presence of facilitating agents such as bacteria and humic acid (*12*−*14*); therefore, the mathematical formulation of these facilitated-transport models was adapted for use in the present study and is only briefly detailed below. The interested reader is directed to the Supporting Information to this paper.

A system of six coupled differential equations was used to represent general rate expressions for the removal of adsorbed HOCs from subsurface systems by surfactant-enhanced processes and to provide temporal and spatial HOC and surfactant distributions in each phase. In the formulation of the mass balance equations, water was assumed to totally cover all other phases such that HOC transfer between phases required passing through the aqueous phase (*12*). A second assumption used in this study was that surfactant monomers in the aqueous phase had a negligible capability for influencing HOC transport relative to the micelles (e.g., refs *10* and *15*). The coupled mathematical equations were solved numerically by a modified Crank−Nicolson scheme (*16*), and concentration-dependent coefficients were decoupled using values calculated in the previous time step (*2, 13*). Flux-type and concentration-type boundary conditions were utilized for the effluent and influent flows, respectively. HOC and surfactant mass balances in each phase were computed and monitored over time using the total flux and the mass within the system.

## Parameter Estimation

To demonstrate the importance of surfactant-enhanced HOC remediation, a representative sandy aquifer column system was modeled. Input parameters for the numerical simulations were as follows: column length ($L$) and diameter ($d$) of 0.1 and 0.025 m, respectively; porosity ($\theta$) of 0.34; bulk solids density ($\rho$) of 1500 kg/$m^3$; solids surface area ($a$) of 3 $m^2$/g; pore velocity ($v$) of 2.71 × $10^{-5}$ m/s; hydrodynamic dispersion coefficient ($D$) of 1.63 × $10^{-8}$ $m^2$/s; time step ($\Delta t$) of 1 s; and nodal spacing ($\Delta x$) of 1 × $10^{-4}$ m. Rate and equilibrium parameters for HOC and surfactant sorption to the model aquifer material and for HOC partitioning to micelles and sorbed surfactants are reported in Table 1; these values are based in part on experimental data reported in our preceding paper (*10*) that have been normalized when necessary for the above solids surface area as suggested by previous studies (*17, 19*). The interested reader is directed to the Supporting Information for complete details of how all rate and equilibrium parameters were estimated.

Empirical equations were developed to fit the highly nonlinear surfactant sorption isotherms on the model aquifer material over the various sorption regions. A single micellar partition coefficient value was used for each HOC and surfactant combination because the isotherms were linear and the coefficients showed only a slight dependence on solute concentration (*10*). Because HOC partition coefficients to sorbed surfactants were highly dependent on the sorbed surfactant concentration, however, an analogous simplification required additional justification. In our simulations, relatively high surfactant doses were utilized as would be expected for a surfactant-enhanced remediation application. Preliminary simulation results showed that use of these high doses minimized the effects of varying HOC partition coefficients to sorbed surfactants, as verified by comparing use of a single coefficient value versus multiple values for SDS and Tween 80; in all cases, there were no significant differences in HOC removal (data not shown). Therefore, in this study only a single average HOC partition coefficient for sorbed SDS and Tween 80 was used as shown in Table 1. Note, however, that for applications using lower surfactant doses (e.g., <10 × cmc), this simplification may not be valid.

First-order model fits to literature data were used to obtain forward rate coefficients for all sorption/partitioning processes. First-order reverse rate coefficients were then estimated from the ratios of forward rate coefficients and the appropriate equilibrium distribution coefficients (*12, 14*). Note that this approach is strictly valid only if sorption/partitioning isotherms are linear. Experimental results for HOC partitioning to micelles and sorbed surfactants showed such linearity (*10*). For surfactant desorption rates, however, the approach could not be utilized directly because of the highly nonlinear sorption isotherms. Instead, the SDS sorption isotherm was regionally linearized and regional distribution coefficients were then used in the analyses. For Tween 80, a Langmuir-type sorption coefficient and a

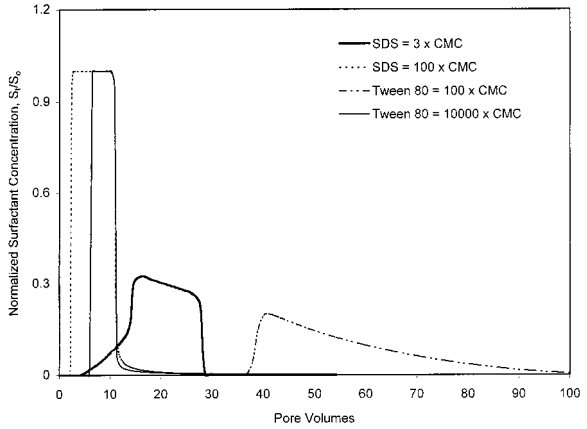


**FIGURE 1. Surfactant breakthrough curves for a pulse width of 5 pore volumes. $S_0$ and $S_t$ are the influent and effluent surfactant concentrations, respectively.**

parameter indicative of the remaining sorption capacity were utilized to determine approximate reverse rate coefficients (*21*).

## Results and Discussion

**Surfactant Transport.** The transport of surfactants in our model sandy aquifer was simulated using the input parameters specified under Parameter Estimation and those shown in Table 1. Normalized breakthrough curves (BTCs) for SDS and Tween 80 are shown in Figure 1. Flushing with lower surfactant concentrations resulted in highly nonsymmetric BTCs due to sorbent−surfactant and surfactant−sorbed surfactant interactions. Nonsymmetric surfactant BTCs and considerable tailing caused by slow release of sorbed surfactants have been reported for the transport of nonionic surfactants through sand columns (*22*); in that study, the authors utilized two hypothetical sorption regimes that depended on the sorbed surfactant concentration and molecular conformation to propose an empirical two-stage sorption kinetic model that considered surfactant monomer−surface and surfactant monomer−sorbed monomer interactions.

When a low SDS concentration (e.g., 3 × cmc) is used, early breakthrough with a low slope (i.e., low normalized concentration) initially appears in the column effluent indicating the low affinity of SDS molecules for the solid phase due to the electrostatic repulsion between the negatively charged SDS molecules and mineral surface. Shortly thereafter, the BTC exhibits a steeper slope due to the higher sorption capacity of the solid phase (isotherm regions II and III, ref *10*) resulting from the interactions among sorbed SDS molecules. Upon flushing with an SDS solution at 100 × cmc, the overall SDS retardation decreases appreciably to a value of ∼2.4 and the normalized concentration approaches 1.0 because the aqueous surfactant mass is much larger than the total sorption capacity (i.e., 165 mg of SDS) of the solid phase in the column. Also, the electrostatic repulsion effect resulting in a nonsymmetric SDS BTC is now absent because sorption by surfactant molecule interactions dominates at high concentrations. When SDS flushing is halted, elution of previously sorbed SDS molecules leads to a long tailing effect; tailing results because of the strong affinity of SDS to the solid phase in regions II and III (i.e., where hemimicelles and admicelles exist) and the subsequent slow release of sorbed SDS.

Flushing with a Tween 80 concentration of 100 × cmc results in a BTC that exhibits a sharp leading edge and significant tailing. This behavior is typical of a Langmuir-type sorption isotherm (*21*) and is attributed to the strong affinity of Tween 80 for the solid phase for these conditions.

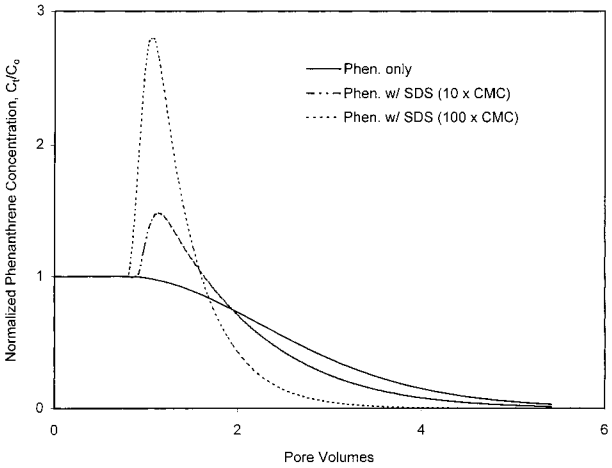


**FIGURE 2. Phenanthrene elution curves for various SDS concentrations (simulations assume no SDS sorption to the aquifer sand). SDS breakthrough reaches 0.5 at 1 pore volume (not shown).**

Note that at this particular dose, the total mass of Tween 80 in the column is ∼21 mg, compared with a total column Tween 80 sorption capacity of 680 mg. When the simulated influent Tween 80 concentration is increased to 10000 × cmc (a physically unrealistic value), the BTC shifts to the left (i.e., less Tween 80 retardation) and the normalized concentration in the effluent increases. However, even at this extremely high concentration (∼13%), the sorption of Tween 80 on the solid phase still has a significant influence on its retardation.

**HOC Transport without Considering Surfactant Sorption.** Many studies that have dealt with facilitated contaminant transport and/or enhanced elution of contaminants did not consider the possible loss of facilitating agents in their models (e.g., *12*); therefore, for our initial simulations we chose to neglect surfactant sorption on the solid phase to quantify the amount of error that would result from this deficiency. To simulate an SER process applicable for removing sorbed contaminants from subsurface systems, HOC concentrations in the effluent ($C_t$) were normalized by the initial aqueous concentration present within the pores ($C_o$, at equilibrium with the sorbed HOC amount, $q_{HOC}$). In Figure 2, phenanthrene elution curves are shown for various influent SDS concentrations. A retardation factor of ∼2.8 can be estimated for phenanthrene in the absence of SDS using the values for $\theta$ and $\rho$ and the distribution coefficient in Table 1. Thus, the elution of phenanthrene by flushing with only water shows a normalized concentration of 0.5 at 2.8 pore volumes and also shows that the majority of phenanthrene is removed from the column within 5 pore volumes (Figure 2). If flushing is instead done with SDS solutions, elution of phenanthrene is enhanced when the sorption of SDS itself is negligible (i.e., the normalized effluent phenanthrene concentration goes above 1.0); enhanced removal results from the solubility of phenanthrene in the mobile micellar phase. In addition, one can see that fewer total pore volumes are needed to remove all of the phenanthrene originally present inside the column. As the influent SDS concentration increases, an increasing number of micelles are available to solubilize the contaminant; thus, desorption is enhanced, and the flushing time required to remove all phenanthrene decreases. Similar results have been previously reported when loss of facilitating agent is not considered (*12*−*14*).

**HOC Transport with Surfactant Sorption.** As stated previously, no significant differences between simulations using a single (average) value versus multiple HOC partition coefficients to sorbed surfactant were observed when high

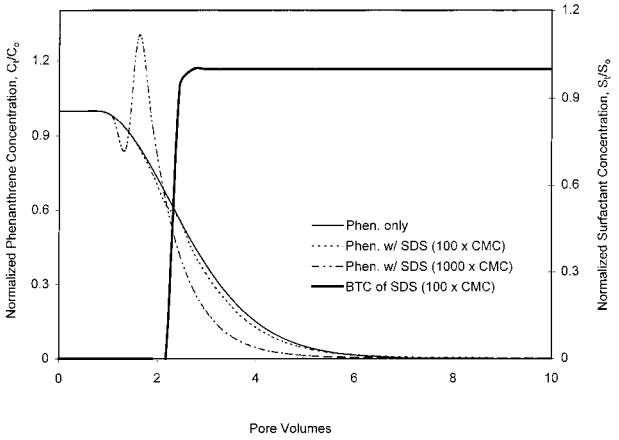


**FIGURE 3. Phenanthrene elution curves for various SDS concentrations. SDS breakthrough reaches 0.5 at ~2.4 pore volumes for a 100 × cmc concentration.**

concentrations of SDS and Tween 80 were used to flush the contaminated porous media. Therefore, the single partition coefficients listed in Table 1 were used for all subsequent simulations.

When surfactant sorption to the solid phase *is* considered, a totally different perspective for phenanthrene removal is obtained (Figure 3). As an SDS concentration of 100 × cmc is flushed into the column, the SDS BTC begins to appear after 2 pore volumes. Because the retardation of phenanthrene is only slightly greater than that of SDS itself, the majority of the phenanthrene originally present in the column is largely unaffected by SDS addition. Only phenanthrene present in the column behind the SDS front (i.e., the SDS mass transfer zone) has the opportunity to partition to the micelles and sorbed SDS. The aqueous phase phenanthrene concentration thus decreases, whereas the phenanthrene partitioned to micelles begins to appear in the effluent. However, the influence of SDS micelles on the phenanthrene elution curve is minimal because of the relatively slow solubilization rate. In addition, the total mobile phenanthrene concentration (i.e., aqueous plus micellar) is less than that without SDS addition because phenanthrene is also partitioned to the sorbed SDS. Even worse, because phenanthrene is present in the sorbed SDS, a longer flushing time is required to totally remove phenanthrene relative to flushing with only water because the tailing effects are more pronounced.

When a higher surfactant concentration (e.g., 1000 × cmc) is used to flush the column, the SDS BTC (not shown in Figure 3) appears sooner and thus a higher micellar partitioning effect is observed. Faster SDS breakthrough results in a larger partitioning of phenanthrene to micelles and sorbed SDS; enhanced phenanthrene removal is achieved due to the relatively higher micellar versus sorbed SDS concentration. However, it should be noted again that the application of such a high surfactant dose may be physically and economically unrealistic.

Because the transport of SDS at 100 × cmc is similar to that of phenanthrene by water, there are no practical benefits obtained by adding it to this system. This observation is even more striking when a contaminant of higher solubility, such as naphthalene, is considered. Because naphthalene is less hydrophobic than phenanthrene, it has a smaller retardation factor (~1.3 in our simulated system). Even when a very high concentration of SDS (1000 × cmc) is used for flushing, there is very little effect on the removal of naphthalene from the column (data not shown). Therefore, the relative affinity of HOCs and surfactants for the solid phase (i.e., the respective retardation factors) is critical for

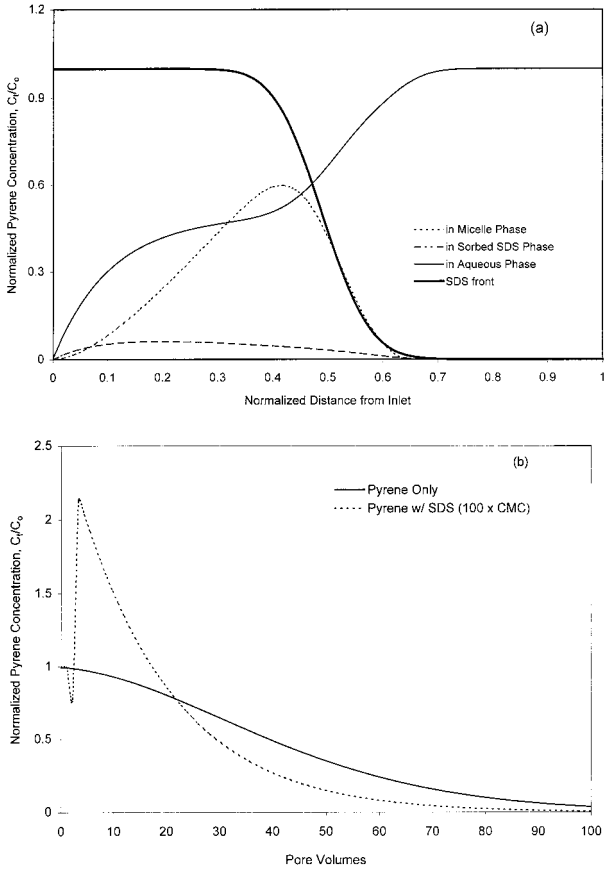


**FIGURE 4. Pyrene elution by SDS (100 × cmc): (a) spatial distribution of pyrene in aqueous, micellar, and sorbed surfactant phases (flushing time = 1.6 pore volumes); (b) pyrene elution curve.**

determining whether contaminant removal can be enhanced by surfactants.

Tween 80 has been suggested for SER applications because it is a food-grade surfactant having both a low toxicity and a high biodegradability (1). However, our simulations with Tween 80 indicated that phenanthrene removal is largely unaffected by even high surfactant concentrations (e.g., 10000 × cmc, data not shown) because Tween 80 sorption occurs well above the cmc (*10*). Because the phenanthrene desorption front moves ahead of the Tween 80 sorption front, phenanthrene appears in the effluent long before Tween 80 breakthrough occurs.

Simulation results for a contaminant more hydrophobic than phenanthrene are shown in Figure 4. A snapshot of the spatial distribution of pyrene (retardation factor of ~43.7 in our simulations) within the one-dimensional column is shown in Figure 4a for the addition of an SDS solution of concentration 100 × cmc. The fronts of SDS micelles and sorbed SDS extend into the column up to a normalized distance of ~0.7 at a flushing time of 100 min (i.e., 1.6 pore volumes). The aqueous phase pyrene located to the right of this point is largely unaffected by the presence of SDS. Up to the middle of the column, most of the pyrene originally adsorbed to the solid phase has been redistributed among the aqueous, micellar, and sorbed surfactant phases. The fraction of pyrene in the aqueous phase is still relatively large due to the slow rates of partitioning to micelles and sorbed surfactant. Near the influent end of the column, the fraction of pyrene present in sorbed SDS is greater than that in micelles because of the relatively slower elution of pyrene from sorbed SDS. Elsewhere, the amount of pyrene in the micellar phase is greater than that in the sorbed surfactant phase because of the high concentration of micelles relative to sorbed SDS.

Thus, the ultimate pyrene distribution is highly dependent on the SDS dose selected because it determines the relative SDS amounts present as micelles and sorbed surfactant. The effect of enhanced pyrene solubilization in the column effluent becomes apparent after 2 pore volumes (Figure 4b); this corresponds to the breakthrough of SDS from the column (not shown in Figure 4b). Pyrene removal from the system is accelerated by partitioning to the mobile micelles, and the overall flushing time necessary for complete contaminant removal is reduced.

On the basis of simulation results for several other contaminants of various hydrophobicities (data not shown), it becomes evident that the greatest enhancement of remediation is achieved when the hydrophobicity of the contaminant increases. In addition, the extent of remediation enhancement depends greatly on the relative retardation of the contaminant to be removed and the surfactant used to flush an aquifer. Another important observation from the simulations is that the elution of HOCs partitioned to sorbed surfactants requires a long remediation time because of the relatively strong affinity of surfactant sorption to soil minerals as well as slow HOC desorption rates. Therefore, any evaluation of SER for the removal of HOCs must be based on a comparison of these important factors. Otherwise, the addition of surfactant into a contaminated aquifer might actually result in exacerbating the problem.

**Sensitivity Analysis.** In the preceding sections, model simulations were conducted to evaluate factors affecting HOC removal based on a contaminated sandy aquifer system. In general, the results showed that sorption interactions of HOCs and surfactants with the solid phase are critical variables in predicting HOC removal. Because the extents and rates of these interactions will be different from site to site depending on subsurface characteristics and the particular contaminants present, the impact of varying important model parameters was examined in detail. Of the variables studied, the effects of slow HOC desorption from the solid phase and the presence of organic matter in the solid phase are briefly discussed below; additional information on their simulations as well as the other model parameters investigated is provided in the Supporting Information.

The immobile solid phase in a subsurface system is composed of a complicated mixture of soil minerals and organic matter that controls the effective rates of HOC sorption and desorption (*23*). Often a two-site model is used to divide the solid phase into two fractions that are reacting either quickly or slowly (i.e., labile versus nonlabile) with respect to HOC sorption/desorption (*24*−*27*). For this study, however, we chose to focus primarily on HOC sorption/desorption rates for the relatively labile soil fraction to evaluate its importance for HOC remediation.

Figure 5 shows the elution of phenanthrene for a 100 × cmc SDS dose when different sorption rates to the solid phase are considered. Because the distribution coefficient is held constant at $4.11 \times 10^{-4}$ L/g (Table 1), relative variations in the forward sorption rate constants apply equally to the desorption rate constants. Thus, it is possible to investigate contaminated systems having extremely slow HOC desorption characteristics resulting from a highly porous solid phase and/or intraorganic matter diffusion (*23*−*28*). Phenanthrene removal under equilibrium desorption conditions ($k_{f,HOC}^{min} = 1.39 \times 10^{-1}\ s^{-1}$) exhibits a very sharp elution curve and shows minimal dependence on the SDS: elution approaches that using only water flushing. However, as phenanthrene sorption/desorption rates decrease, the temporal distribution of phenanthrene in the mobile phase has a flatter (i.e., more dispersive) shape, indicating that more interactions with micelles and sorbed SDS are now possible. For a sorption rate constant $k_{f,HOC}^{min} = 1.39 \times 10^{-4}\ s^{-1}$, aqueous phase phenanthrene is greatly affected by SDS micelles and sorbed

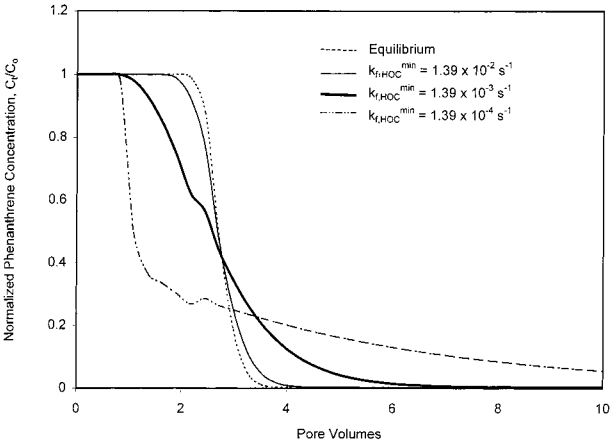


**FIGURE 5. Effect of phenanthrene sorption/desorption rates on the phenanthrene elution curve (SDS = 100 × cmc). For the equilibrium condition, $k_{f,HOC}^{min} = 1.39 \times 10^{-1}\ s^{-1}$.**

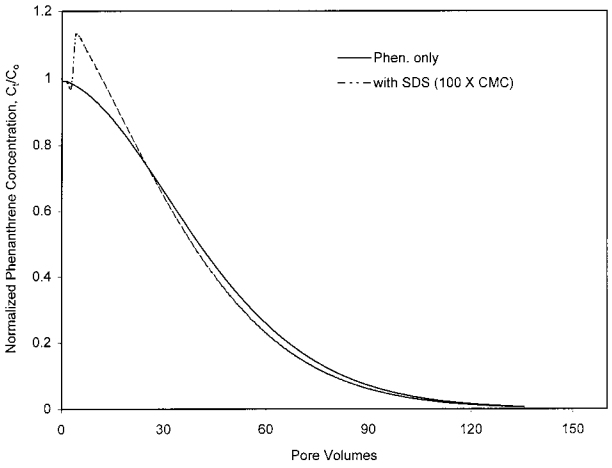


**FIGURE 6. Effect of soil organic matter on the phenanthrene elution curve (SDS = 100 × cmc). $K_D$ ($\equiv K_{HOC}^{min}$) = 0.01 L/g.**

SDS; the effluent phenanthrene concentration (aqueous plus micellar) shows an initial rapid drop because a large fraction of phenanthrene partitions to sorbed SDS. Thereafter, a very long tailing of phenanthrene occurs in the effluent because of the slow release of phenanthrene from sorbed SDS.

A final series of simulations were performed to consider the impact of native organic matter on phenanthrene removal; in these tests, the subsurface solid phase was assumed to have an organic carbon content of 0.118% ($f_{oc}$ = 0.00118) and a phenanthrene distribution coefficient of 0.01 L/g (*29*). Because the forward phenanthrene sorption rate coefficient used in our previous simulations is comparable to that reported for the labile fraction of similar subsurface materials (*23*, *24*), we chose to continue using this value ($k_{f,HOC}^{min} = 1.39 \times 10^{-3}\ s^{-1}$, Table 1). Additionally, although solid phase organic matter may affect surfactant sorption in real subsurface systems, we continued to use the same values for SDS sorption (Table 1) because of the lack of predictive capabilities (*30*, *31*). Results of the simulations are shown in Figure 6. The larger solid phase distribution coefficient now requires a much longer flushing time with water to remove phenanthrene (i.e., compare with Figure 2). When an SDS dose of 100 × cmc is used for flushing, enhanced elution is observed in the column effluent because the retardation of SDS is now smaller than that of phenanthrene. It is noteworthy that the distribution coefficient of phenanthrene to this solid phase having $f_{oc}$ = 0.00118 is comparable to that of pyrene to the model sandy aquifer (Table 1). However, from a comparison of Figure 6 with Figure 4b, it

is clear that the enhancement effect of SDS is much greater for pyrene than it is for phenanthrene, primarily because the micellar partition coefficient of pyrene is larger than that of phenanthrene.

In addition to the effects of reversible HOC sorption processes from the immobile solid phase as shown in Figure 6, the possibility of irreversible sorption or resistant desorption (e.g., attributed to the organic matter; refs *32* and *33*) may need to be considered. For the latter case, previous studies have suggested that the HOC distribution coefficient has a linear relationship with the desorption-resistant reactive fraction of a soil (*33*); this effect then leads to a desorption distribution coefficient that is larger than the forward sorption distribution coefficient. For our systems, consideration of this type of an effect results in a much longer tailing of phenanthrene in the effluent and a significantly longer flushing time than that seen in Figure 6 (data not shown). Finally, the potential effect of surfactants on the HOC desorption rate coefficient (*34, 35*) was not considered in this study because it is not clear how important the effect might be in a real subsurface system.

The important rate and equilibrium parameters evaluated here can provide useful guidelines for the design and application of SER processes for subsurface systems contaminated with HOCs. To provide a truly realistic analysis of SER effectiveness, site-specific data including important HOC and surfactant rate processes must be available for input to the mathematical model. Without this information and proper analysis, addition of surfactant solutions may actually result in decreased performance and longer remediation times. Selection of an appropriate surfactant (i.e., one with a high HOC solubilization capability and a low solid phase sorption potential) will be critical in the ultimate success of SER applications.

## Acknowledgments

We gratefully acknowledge two reviewers who provided constructive comments for improving the manuscript. Preliminary funding for this work was provided by the Office of the Vice President for Research and Associate Provost for Graduate Studies, through the Center for Energy and Mineral Resources, Texas A&M University. Additional funding was provided by the Gulf Coast Hazardous Substance Research Center, which is supported under cooperative agreement R822721-01-4 with the U.S. Environmental Protection Agency. The contents of this paper do not necessarily reflect the views and policies of the U.S. EPA nor does the mention of trade names or commercial products constitute endorsement or recommendation for use.

## Supporting Information Available

Detailed information on the development of the one-dimensional transport model, the parameter estimation procedures utilized to obtain the values shown in Table 1, and the parameter sensitivity analysis (14 pages). Ordering information is given on any current masthead page.

## Literature Cited

(1) Pennell, K. D.; Abriola, L. M.; Weber W. J. *Environ. Sci. Technol.* **1993**, *27*, 2332−2340.
(2) Abriola, L. M.; Dekker T. J.; Pennell, K. D. *Environ. Sci. Technol.* **1993**, *27*, 2341−2351.
(3) Abdul, A. S.; Ang, C. C. *Ground Water* **1994**, *32*, 727−734.
(4) Abdul, A. S.; Gibson, T. L.; Rai, D. N. *Ground Water* **1990**, *28*, 920−926.
(5) Shiau, B.-J.; Sabatini, D. A.; Harwell, J. H. *Ground Water* **1994**, *32*, 561−569.
(6) Mason, A. R.; Kueper, B. H. *Environ. Sci. Technol.* **1996**, *30*, 3205−3215.
(7) Abriola, L. M., et al. In *Surfactant-Enhanced Subsurface Remediation*; Sabatini, D. A., Knox, R. C., Harwell, J. H., Eds.; American Chemical Society: Washington, DC, 1995; pp 10−23.
(8) Freeze, G. A., et al. In *Surfactant-Enhanced Subsurface Remediation*; Sabatini, D. A., Knox, R. C., Harwell, J. H., Eds.; American Chemical Society: Washington, DC, 1995; pp 191−200.
(9) Edwards, D. A.; Adeel, Z.; Luthy, R. G. *Environ. Sci. Technol.* **1994**, *28*, 1550−1560.
(10) Ko, S.-O.; Schlautman M. A.; Carraway, E. R. *Environ. Sci. Technol.* **1998**, *32*, 2769−2775.
(11) Jafvert, C. T. *Environ. Sci. Technol.* **1991**, *25*, 1039−1045.
(12) Enfield, C. G.; Bengtsson, G. *Ground Water* **1988**, *26*, 64−70.
(13) Corapcioglu, Y. M.; Jiang, S. *Water Resour. Res.* **1993**, *29*, 2215−2226.
(14) Johnson, W. P.; Amy, G. L.; Chapra, S. C. *J. Environ. Eng.* **1995**, *121*, 438−446.
(15) Nayyar, S. P.; Sabatini, D. A.; Harwell, J. H. *Environ. Sci. Technol.* **1994**, *28*, 1874−1881.
(16) Fletcher, C. A. J. *Computational Techniques for Fluid Dynamics I*, 2nd ed.; Springer-Verlag: Berlin, 1991.
(17) Huang, W.; Schlautman, M. A.; Weber, W. J. *Environ. Sci. Technol.* **1996**, *30*, 2993−3000.
(18) Karcher, W. W. *Spectral Atlas of Polycyclic Aromatic Compounds Including Data on Physico-Chemical Properties, Occurrence and Biological Activity*; Kluwer Academic Publishers: Boston, 1988; Vol. 1.
(19) Schwarzenbach, R. P.; Gschwend, P. M.; Imboden, D. M. *Environmental Organic Chemistry*; Wiley: New York, 1993.
(20) Schlautman, M. A.; Morgan, J. J. *Environ. Sci. Technol.* **1994**, *28*, 961−969.
(21) Weber, W. J.; Pennell, K. D.; Dekker: T. J.; Abriola, L. M. In *Recent Advances in Groundwater Pollution Control and Remediation*; Aral, M. M., Ed.; Springer-Verlag: New York, 1998; in press.
(22) Adeel, Z.; Luthy, R. G. *Environ. Sci. Technol.* **1995**, *29*, 1032−1042.
(23) Weber, W. J.; Huang, W. *Environ. Sci. Technol.* **1996**, *30*, 881−888.
(24) Karickhoff, S. W. In *Contaminants and Sediments*; Baker, R. A., Ed.; Ann Arbor Science Publishers: Ann Arbor, MI, 1980; Vol. II, pp 193−205.
(25) Karickhoff, S. W. *Environ. Toxicol. Chem.* **1985**, *4*, 469−479.
(26) Di Toro, D. M.; Horzempa, L. M. *Environ. Sci. Technol.* **1982**, *16*, 594−602.
(27) Pignatello, J. J. *Environ. Toxicol. Chem.* **1990**, *9*, 1117−1126.
(28) Ball, W. P.; Roberts, P. V. *Environ. Sci. Technol.* **1991**, *25*, 1237−1249.
(29) Huang, W.; Young, T. M.; Schlautman, M. A.; Yu, H.; Weber, W. J. *Environ. Sci. Technol.* **1997**, *31*, 1703−1710.
(30) Hand, V. C.; Williams, G. K. *Environ. Sci. Technol.* **1987**, *21*, 370−373.
(31) Brownawell, B. J.; Chen, H.; Zhang, W.; Westall, J. C. *Environ. Sci. Technol.* **1997**, *31*, 1735−1741.
(32) Pavlostathis, S. G.; Mathavan, G. N. *Environ. Sci. Technol.* **1992**, *26*, 532−538.
(33) Deitsch, J. J.; Smith, J. A. *Environ. Sci. Technol.* **1995**, *29*, 1069−1080.
(34) Sahoo, D.; Smith, J. A. *Environ. Sci. Technol.* **1997**, *31*, 1910−1915.
(35) Smith, J. A.; Jaffe, P. R.; Chiou, C. T. *Environ. Sci. Technol.* **1990**, *24*, 1167−1172.
(36) Holsen, T. M.; Taylor, E. R.; Seo, Y.-C.; Anderson, P. R. *Environ. Sci. Technol.* **1991**, *25*, 1585−1589.
(37) Dulfer, W. J.; Bakker, M. W. C.; Govers, H. A. J. *Environ. Sci. Technol.* **1995**, *29*, 985−992.
(38) Grazel, M.; Thomas, J. K. *J. Am. Chem. Soc.* **1973**, *95*, 6885−6889.

*Received for review December 12, 1997. Revised manuscript received June 9, 1998. Accepted June 29, 1998.*

ES9710767